AD-A055 627 AIR FORCE INST OF TECH WRIGHT-PATTERSON AFB OHIO SCH--ETC F/G 18/8
EFFECTS OF NEUTRON RADIATION ON ALUMINUM-GALLIUM-ARSENIDE LASER--ETC(U).
MAR 78 T E WALSH

UNCLASSIFIED AFIT/GNE/PH/78-11 NL

1 OF 1
ADA
055627

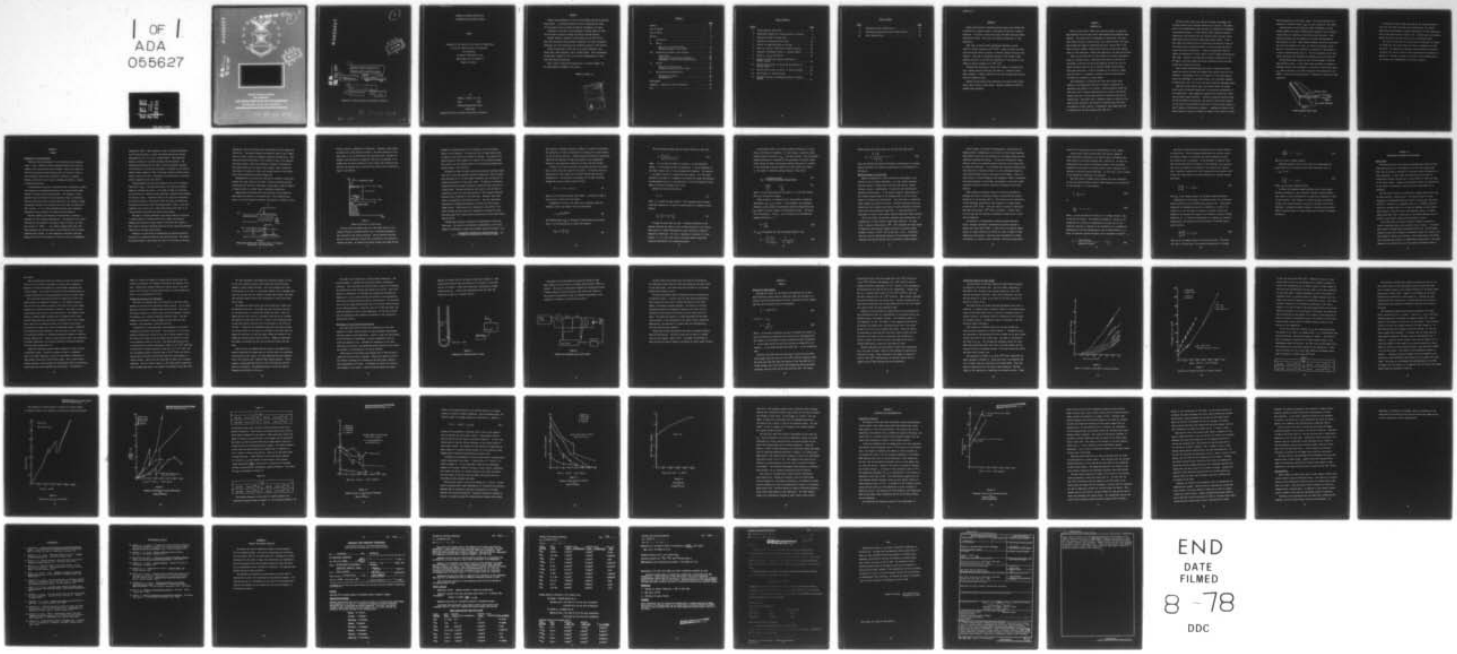

END
DATE FILMED
8-78
DDC

UNITED STATES AIR FORCE

AIR UNIVERSITY

AIR FORCE INSTITUTE OF TECHNOLOGY

Wright-Patterson Air Force Base, Ohio

(6) EFFECTS OF NEUTRON RADIATION ON ALUMINUM-GALLIUM-ARSENIDE LASERS.

THESIS

(14) AFIT/GNE/PH/78-11

(10) Thomas E. (Edward) Walsh, Jr.
Capt USAF

(9) Master's thesis,

(11) Mar 78

(12) 65p.

Approved for public release; distribution unlimited.

Ø12 225

cat

EFFECTS OF NEUTRON RADIATION ON ALUMINUM-GALLIUM-ARSENIDE LASERS

THESIS

Presented to the Faculty of the School of Engineering

of the Air Force Institute of Technology

Air University

in Partial Fulfillment of the

Requirements for the Degree of

Master of Science

by

Thomas E. Walsh, Jr., B.S.

Capt USAF

Graduate Engineering Physics

March 1978

Preface

Captain Armen Mardiguan of the Air Force Weapons Laboratory proposed this project. I am deeply indebted to him for supplying the lasers for this project and for giving his support throughout its course.

Gratitude is also due to the Department of Energy (DOE) for funding the reactor operation through the Reactor Sharing Program.

Special thanks is extended to Brian Hajek and the staff of the Ohio State University Nuclear Reactor Laboratory for their invaluable assistance with the irradiation and activation aspects of this project.

A debt of gratitude is also owed to my faculty advisors, Drs. George John, Robert Henghold, and G. Richard Hagee. Their willingness to help when I needed it, and to let me work independantly at other times was greatly appreciated.

Last, I want to express my appreciation to my wife, Sandra, for her encouragement throughout this project.

Thomas E. Walsh, Jr.

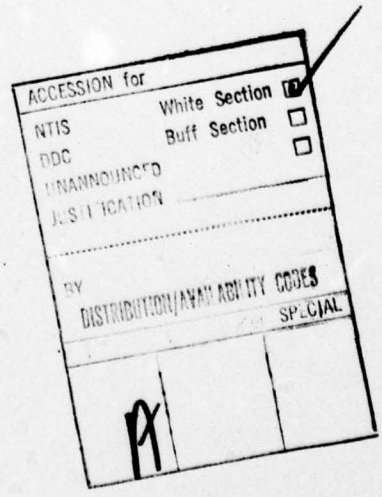

Contents

		Page
Preface		ii
List of Figures		iv
List of Tables		v
Abstract		vi
I.	Introduction	1
II.	Theory	5
	Operation of Injection Lasers	5
	Radiation Damage to Laser Diodes	13
III.	Experimental Equipment and Procedures	18
	Laser Diodes	18
	Irradiation Facilities and Procedures	20
	Measurement of Laser Diode Characteristics	22
IV.	Results	26
	Neutron Flux Measurements	26
	Irradiation Effects on Laser Diodes	28
V.	Discussion and Recommendations	41
	Discussion of Results	41
	Recommendations	45
Bibliography		47
Appendix A:	Request for Reactor Operation	49
Vita		55

List of Figures

Figure		Page
1	Stripe Geometry Laser Diode	3
2	Energy Band Diagram for a Heavily Doped p-n Junction . .	7
3	Density-of-States for Laser Diode	8
4	Apparatus for Measuring Power Output	23
5	Circuit for Measuring Power and Voltage	24
6	Power vs. Current of RCA #550 at Several Fluences	29
7	Increase In Threshold Current vs. Neutron Fluence	30
8	Power vs. $(I-I_{th})$ for RCA #65	33
9	Change in Differential Quantum Efficiency vs. Neutron Fluence	34
10	Relative Power Output at 100 mA Above Threshold vs. Neutron Fluence	36
11	Relative Power Output at 200 mA vs. Neutron Fluence . . .	38
12	Bias Voltage vs. Forward Current	39
13	Estimated Increase in Threshold Current vs. Neutron Fluence	42

List of Tables

Table		Page
I	Threshold Current Damage Factors	31
II	Differential Quantum Efficiency Damage Factors	35
III	Power Damage Factors	35

Abstract

Double heterojunction aluminum-gallium-arsenide laser diodes were irradiated in a nuclear reactor to determine the effects of neutron radiation. Two types of lasers were used, RCA C30127 and Laser Diode Laboratories LCW-10. Both types can operate continuously at room temperature.

Both types of diodes showed significant decreases in power output at neutron fluences of 10^{14} n/cm^2. Linear increases in threshold current and linear decreases in external quantum efficiency were observed. There was no significant change in bias voltage versus forward current or in the spectral composition of the outputs of the diodes at neutron fluences up to 10^{15} n/cm^2.

Formulas were developed to predict the changes in threshold current, external quantum efficiency and power at a constant current above threshold. Damage coefficients for these formulas were derived from the irradiation data.

Unusual discontinuities were observed in the power output versus input current curves of some diodes. Neutron irradiation tended to enhance these anomalies.

CHAPTER I

INTRODUCTION

Since the first laser diodes were announced almost 15 years ago, many advances have been made toward understanding and optimizing their behavior. The lasers have the advantages of being small, and since they convert electrical power directly into coherent light, the output may be modulated simply by modulating the input current (Ref 17:42). Until recently, however, these devices could not be operated continuously at room temperature, making them impractical for many applications.

Since the Air Force may use laser diodes in a nuclear environment, there is a definite need to understand the effects of radiation on the (AlGa) as devices with OH stripe geometry because they are currently the best suited for use in optical communications systems. This study along with a study by Ackermann on the effects of gamma radiation (Ref 1) is designed to provide a better understanding of the effects of radiation on these diodes.

The development of continuous wave (CW) laser diodes which operate at room temperature has been a process of improving the efficiency and quality of the devices. Gallium-arsenide (GaAs) and some other III-IV compound semiconductors are used for the devices because they have a direct gap between the conduction band and the valence band. This means that no momentum change is required in the band-to-band transition, and radiative transitions may occur with the emmision of only a photon. Consequently, much higher gain can be achieved for the same pumping level (Ref 12:4).

The first laser diodes were made by diffusing an acceptor into a heavily doped n-type substrate forming a p-n junction. The thickness of the recombination region was kept to a minimum by introducing a steep doping profile. An even thinner active region was made by depositing p-type material onto the substrate with a process called vapor phase epitaxy and later liquid phase epitaxy (LPE). It was then found that aluminum could be substituted for gallium in some of the lattice sites of gallium-arsenide to raise the band gap and decrease the index of refraction. A layer of degenerately doped p^+ (AlGa) was deposited on a thin p layer to form a single heterojunction (SH) laser. Because of the decrease in index of refraction in the p^+ region, the active region was better confined and there was less optical loss outside the cavity.

Later, double heterojunctions were used to confine the active region even better and give the designer more precise control of its thickness. Additionally, the use of (AlGa)As in the active region allows the wavelength of the emitted light to be controlled somewhat by varying the ratio of Al to Ga, and thus varying the band-gap energy.

Even with active regions only a few microns thick, the diodes still could not dissipate enough heat to be operated continuously at room temperature. Room temperature operation was achieved by confining the active region laterally. Instead of injecting carriers along the entire width of the junction, the injection current was confined to the center of the junction by the use of a narrow stripe contact on the p^+ region as illustrated in figure 1. Limiting the volume of the active region in this way, allowed the volume of the crystal to accept

the heat generated in the active region. The stripe geometry also reduced the threshold current (I_{th}) for laser operation. (Ref 8:109)

Although much work has been done toward development of laser diodes suitable for optical communications systems, very few studies of the effects of radiation on the devices have been done. Early radiation-effects work was designed to increase understanding of the properties of GaAs. These studies examined the optical properties the electrical behavior of a GaAs p-n junction (Auckerman, et al, Ref 2), or the effect of irradiation on operation of GaAs lasers at or below threshold (Barnes, Ref 4). The only extensive work on GaAs lasers operating above threshold was Southward and others (Ref 19).

The Southward study dealt with fast neutron damage of diffused GaAs injection lasers. In the report they discussed an increase in threshold current with irradiation, a reduction in power output above I_{th}, and an increase in the delay associated with modulation of the diodes. They also discussed effects of temperature variation on these quantities.

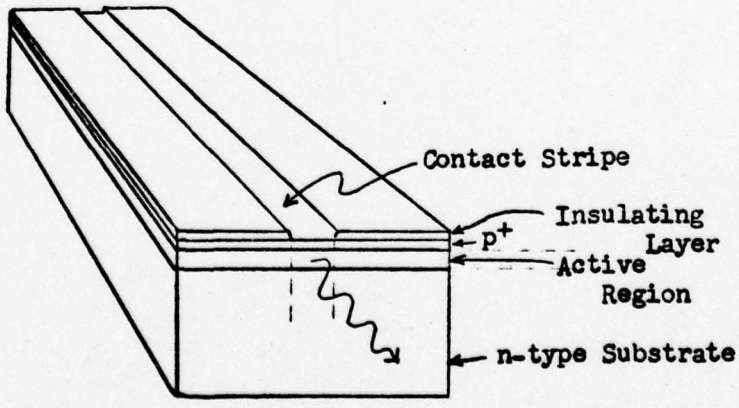

Figure 1

Stripe Geometry Laser Diode

Two brands of laser diodes were used for the study presented in this work, RCA C30127 and Laser Diode Laboratories, Inc. LCW-10. Both devices are designed to operate continuously at room temperature with a peak radiant power of about 15 mW. The RCA laser is a developmental type while the Laser Diode Labs is a production model.

The theory of operation for these devices is presented in Chapter II, along with theoretical models for neutron degradation of their operation. The experimental equipment and procedures are described in Chapter III, and the results of the experiments are presented in Chapter IV. Chapter V contains a discussion of the significance of the results and recommendations for further research.

CHAPTER II

THEORY

Operation of Injection Lasers

There are three requirements for the operation of an injection laser. First, a medium in which stimulated emission will occur is needed so that optical gain can be produced. Next, there must be a cavity with partially reflecting ends that will cause the light to pass through the medium until sufficient intensity is achieved. Finally, there must be some method of pumping the medium to achieve a population inversion.

In semiconductor materials, transitions such as absorption, spontaneous emission, and stimpulated emission occur between energy bands instead of between discrete energy levels. The bandgaps in semiconductors may be divided into two categories, direct and indirect. Electron transitions across a direct band gap do not require a change in momentum, therefore the transition may occur with the emission of only a photon. It is in direct bandgap materials that stimulated emissions may occur readily, and lasing has been observed.

The most commonly used material for diode lasers is gallium-arsenide, an III-V compound semiconductor. The minimum of the conduction band and the maximum of the valence band are both at the same wave vector, $\overline{k} = [000]$, so a direct bandgap exists (Ref 12:3). Other properties of GaAs also make it well suited for use in optical communications systems. At room temperature, GaAs has a band gap energy of about 1.35 eV and emits at 0.83 μm to 0.91 μm, depending on

doping (Ref 5:291). When aluminum is used to replace some gallium in the crystal lattice, it lowers the energy gap and the emitted wavelength to 0.63 μm to 0.90 μm (Ref 5:291). This makes the material suitable for use with existing infra-red dectors. The wavelength of emission may be tuned to the best response frequency of the detector by varying the percentage of aluminum in the lattice. Another useful property of GaAs is the short carrier lifetime, which causes a fast on-off time. Consequently the GaAs lasers can be modulated at megahertz rates (Ref 12:81).

Gallium-arsenide crystals lend themselves very well to making a Fabry-Perot cavity. The reflective ends of the cavity are formed simply by cleaving the crystal. The change in index of refraction at the crystal-air interface causes sufficient reflection and feedback for lasing to occur. Transverse modes in the cavity are suppressed by sawing the edges of the device to make the sides non-reflecting. The Fabry-Perot cavity, aside from being simple to form, is the most efficient type of cavity for a laser diode because the light is reflected directly back along the narrow active region.

The light is further contained in the active region by situating it between layers of (AlGa)As which have a higher percentage of aluminum and therefore a higher index of refraction (see figure 1). This forms an effective waveguide along the active region and minimizes losses out of the side of the cavity.

Pumping in a laser diode is accomplished by injecting electrons across the p-n junction, hence the term injection laser. The lasers are usually doped so that either the n-type or the p-type or both are

degenerate; that is, the Fermi level lies within the band (figure 2a) (Ref 19:24). The barrier between the conduction band in the n region and that in the p region is reduced by applying a forward bias. This causes electrons from donors in the n region to flow, or be injected, into the p region. This action produces a surplus of electrons in the conduction band at the edge of the p region, which, along with the surplus of vacancies or holes that already exists in the valence band, form a population inversion (figure 2b).

Recombination of the holes and electrons by radiative transitions produces the light output of the laser. There are several possible transitions that may occur radiatively, band-to-band, band-to-acceptor or donor-to-band, or various types of tunneling transitions.

Band-to-band transitions occur when electrons in the conduction band combine with holes in the valence band. This transition may result in a photon emission (radiative transition) or a phonon or free

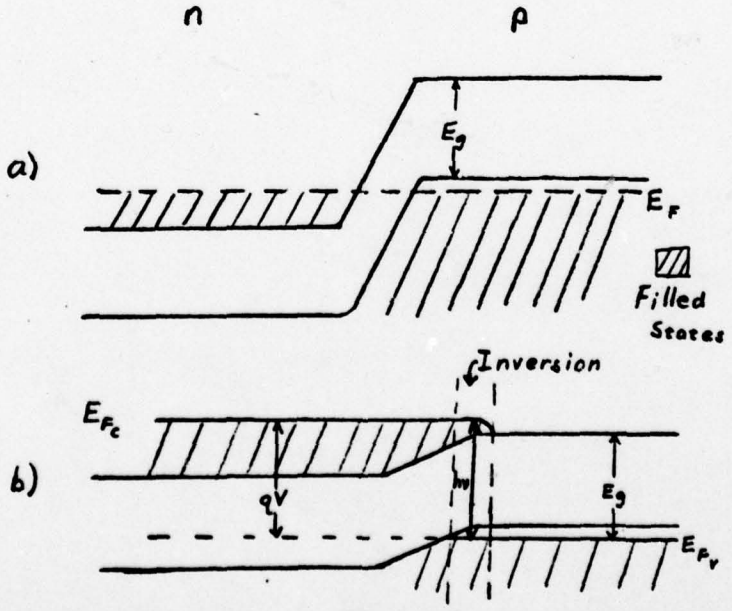

Figure 2

Energy Band Diagram for a Heavily Doped p-n Junction
(a) No Bias (b) Forward Bias

electron emission (nonradiative transition). Generally, laser diodes are doped with a high density of donors. The donor material on the p side causes a tail of states below the conduction band. Because the energy of emitted photons is generally less than the band-gap, it is thought that the lasing transition occurs between the conduction band tail and the impurity level just above the valence band as depicted in figure 3 (Ref 20:696).

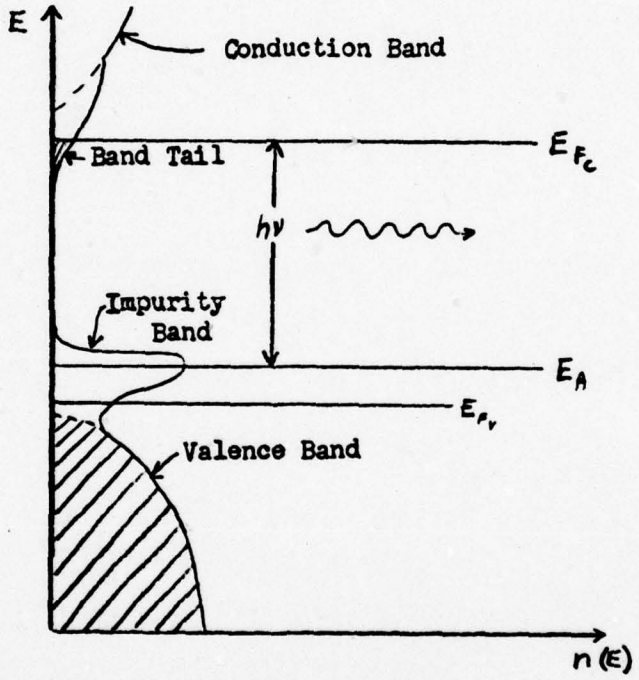

Figure 3

Density-of-States for Laser Diode

The fact that the emission peak of a GaAs laser shifts as the applied voltage is increased implies that a tunneling mechanism is also involved in the lasing transition. Photon assisted tunneling may occur when sufficient forward bias is applied to the junction to uncross the bands. An electron can tunnel through the energy barrier

between the conduction band of the n material into the forbidden region of the p material. It then drops into an empty valence band or impurity level state, and a photon is emitted. The energy of the photon emitted by this process is a function of the applied voltage. This accounts for the observed shift in the emission wavelength with applied energy. (Ref 19:22-23)

Although the band-to-acceptor and photon-assisted tunneling transitions are not the only possible radiative transitions, they are generally considered to be the most likely candidates for the majority of radiative processes in a GaAs laser diode. In addition to radiative transitions there are many nonradiative transitions that may occur in a laser diode. The same transitions that result in the emission of a photon may also occur with the emission of other energy-conserving particles such as phonons or free electrons. Moreover, many other types of nonradiative transitions may occur. The most significant nonradiative recombination processes are those that involve deep energy levels. Transitions due to tunneling to deep levels or between the band and deep levels are nonradiative processes and have been associated with crystal lattice dislocations in GaAs laser diodes (Ref 11:53-54).

During laser operation, radiative and nonradiative transitions both occur. The ratio of the radiative recombinations to the total number of transitions is called the internal quantum efficiency (η_i):

$$\eta_i = \frac{\text{\# radiative recombinations (photons emitted)}}{\text{\# radiative recombinations +\# nonrad. recomb.}} \quad (1)$$

This quantity, although difficult to measure, is useful in describing the operation of a laser, particularly in relating the current density (J) to the optical gain (g). Internal quantum efficiencies approaching 100% have been observed in GaAs laser diodes at low temperatures. Values for room temperature operation are about 50% (Ref 20:708).

In order for a laser to operate, the optical gain per unit length must at least equal the losses in the cavity. The losses consist of absorptions per unit length (α) and losses through the ends with reflectivity R. The decrease in intensity (I) of light traveling through the cavity is given by (Ref 16:3-32).

$$dI = - \alpha I \, d x + g I \, d x \tag{2}$$

where g is the optical gain per unit length. A fraction of light R will be lost at each end of the cavity.

Integration of net loss (or gain) over a complete round trip through a cavity with length L gives the expression

$$I = I_o \, R^2 \, e^{2gL-2\alpha L} \tag{3}$$

The threshold gain (g_{th}) is obtained by substituting the relationship $I = I_o$ and solving for g to give the relation

$$g_{th} = \alpha + \frac{1}{L} \ln \frac{1}{R} \tag{4}$$

The relationship between gain and current density is (Ref 12:8)

$$g = \frac{c^2 \eta_i J^b}{8 \pi q \eta^2 \nu^2 \Delta \nu d} \tag{5}$$

where c is the speed of light in a vacuum, q is the electronic charge, η is the material index of refraction, ν is the frequency of the light emitted, and $\Delta\nu$ is the recombination linewidth. The exponent b is equal to unity for a simple two-level system. In a real semiconductor, the value of b depends on the density of states distribution. No experimental value of b has been found, so for the purposes of this paper, it will be considered to be unity.

Equation (5) may be rewritten as

$$g = \beta J \tag{6}$$

where β is called the gain constant. This expression may be substituted into equation (4) to give the relationship for threshold current density,

$$J_{th} = \frac{1}{\beta} \left(\alpha + \frac{1}{L} \ln \frac{1}{R} \right) \tag{7}$$

It should be noted that the term α includes absorption in the regions adjoining the cavity as well as those occurring in the cavity. Each region in a double heterojunction laser diode has a different absorption coeeficient. The term α appearing in equation (7) incorporates α_1, α_2, and α_3 for each of the three regions along with functions determined by the waveguide geometry.

As mentioned earlier, the internal quantum efficiency of a laser diode is difficult to determine. For this reason, a quantity called external quantum efficiency (η_{ext}) has been defined. Just as internal quantum efficiency is a measure of the percentage of radiative transitions inside the diode, the external quantum efficiency is a measure of the percentage of photons emitted by a laser diode with respect to the number of electrons passing through it (Ref 19:44).

$$\eta_{ext} = \frac{\text{\# photons emitted}}{\text{\# electrons passing through device}} \tag{8}$$

$$= \frac{P/h\nu}{I/\delta} = \frac{P}{IV_i} \tag{9}$$

where P is the output power of the device, I is the bias current, and V_i is the junction voltage.

Below threshold, the emission from a laser diode is primarily spontaneous, and η_{ext} is small. Above threshold, the stimulated emissions quickly render the spontaneous emission insignificant and η_{ext} ideally increases linearly with increasing current. The slope of the increasing P versus I curve is known as the differential quantum efficiency ($\Delta\eta$).

$$\Delta\eta = \frac{\Delta P}{V_i \Delta I} \tag{10}$$

If η_{ext} is considered for only stimulated emission, then

$$\Delta\eta = \frac{(P - P_{th})}{(I - I_{th})\, V_i} = \frac{P}{(I - I_{th})\, V_i} \tag{11}$$

Using assumptions stated before, one can show that (Ref 19:44)

$$\Delta\eta = \eta_i \frac{\frac{1}{L} \ln \frac{1}{R}}{\alpha + \frac{1}{L} \ln \frac{1}{R}} \tag{12}$$

Thus, the differential quantum efficiency is proportional to internal quantum efficiency and inversely proportional to the absorptions in the device.

Radiation Damage to Laser Diodes

Neutron irradiation of a GaAs crystal may cause damage to the crystal by any of several mechanisms. If a fast neutron interacts with the crystal, it might knock atoms from the lattice, thereby leaving a vacancy. Additionally, the atom that was removed may be deposited interstitially. If the neutron energy is large enough, it can transfer enough energy to the displaced atom to set up an avalanche of vacancies and interstitials. This would leave a relatively large damaged area within the crystal. Neutrons interacting with the crystal may also transmute some atoms by neutron absorption reactions which would create additional impurities. A final possibility is ionization of lattice atoms thereby creating additional charge carriers.

Two of the effects of neutrons, ionization and transmutation, are insignificant in their effect on laser diode operation. The high level of impurity doping (about 10^{18} / cm^3) overpowers the small amount of impurities that would be produced by neutron activation (upper estimate is about 5×10^{14} / cm^3 in this experiment). Ionizations that occur are not significant because the free electrons quickly recombine with ionized centers until equilibrium is again reached.

Lattice damage in the form of displacements, interstitials and dangling bonds is significant in its effect on laser diode operation. These defects cause local perturbations in the energy levels and form additional recombination centers. If these are nonradiative recombination centers, the internal quantum efficiency of the device will be expected to decrease. If the centers give radiative recombinations, then there may be radiation produced at a new wavelength because of the displaced energy levels in the region of the damage. Other possible effects of lattice damage include changes in index of refraction, increased absorption or scattering, and changes in electrical properties such as carrier lifetime, electrical resistance, and carrier mobility.

Early studies of radiation effects in GaAs were performed by Aukerman and others to determine changes in electrical and optical properties of the material (Ref 2). They found that the conductivity of GaAs decreased significantly after exposure to a large fluence of neutrons (10^{17} n/cm^2). They also found an increase in absorption band edge with moderate (10^{16} n/cm^2) irradiation. Another result of this study was the discovery of additional energy levels in GaAs after irradiation.

In addition to the mechanisms of physical damage described before, Aukerman referenced a phase-change reaction proposed by Edwards and others (Ref 2:3598). A fast neutron may deposit enough energy in a small volume of the crystal to create a packet of high temperature and pressure. This will cause the material to change irreversibly to a metallic phase creating a relatively large pertur-

bation in the energy levels of the semiconductor in that region.

A more recent study by Barnes dealt with neutron damage in close-confinement (referring to the active region confinement) GaAs laser diodes at and below threshold (Ref 3 and Ref 4). He found, by using diodes with cavities of different lengths, that the primary mechanism for increases in threshold current after irradiation was a decrease in internal quantum efficiency. In his study, little increase in the absorption coefficient was indicated.

The basic model for damage used by Barnes (and later Southward) is that the neutron fluence causes a linear increase in the reciprocal of the lifetime (τ) of the carriers:

$$\frac{1}{\tau} = \frac{1}{\tau_o} + K \phi \tag{13a}$$

or

$$\frac{\tau_o}{\tau_{(\phi)}} - 1 = \tau_o \; K \; \phi \tag{13b}$$

where τ_o is the unirradiated lifetime, K is a damage constant, and ϕ is the neutron fluence. The radiative lifetime is a measure of the probability of a radiative recombination occurring, and the non-radiative lifetime is a measure of the probability of a nonradiative recombination occurring (Recombination rate is proportional to $\frac{1}{\tau}$). Thus, the internal quantum efficiency can be expressed in terms of τ :

$$\eta_i = \frac{\text{total lifetime}}{\text{radiative lifetime}} = \frac{\tau}{\tau_R} \tag{14}$$

The centers formed by neutron irradiation may be either radiative or nonradiative. From the preceding discussion and from the results of previous studies, it is evident that more nonradiative centers are formed and the η_i decreases. If the decrease in radiative lifetime is much less than the decrease in total lifetime, τ_R in equation (14) can be considered to be constant in the presence of a neutron flux. Therefore, equation (14) can be substituted into equation (13b) to give the relationship for neutron degradation of internal quantum efficience:

$$\frac{\eta_i\ (o)}{\eta_i\ (\phi)} - 1 = \tau_o\ K_{\eta i}\ \phi \tag{15}$$

where $K_{\eta i}$ is the damage constant for internal quantum efficience.

Expressions for the changes in threshold current and differential quantum efficience may be derived using equation (15). Since Barnes found that the degradation was due to a decrease in η_i and not an increase in α, all the terms in equation (7) except β may be considered to be constant with respect to an increase in neutron fluence. Therefore, as β is directly proportional to η_i making I_{th} inversely proportional, the expression for the increase in threshold current may be written:

$$\frac{I_{th}\ (\phi)}{I_{th}\ (o)} - 1 = \tau_o\ K_I\ \phi \tag{16}$$

where K_I is the damage constant for threshold current. From equation (12) it is seen that $\Delta\eta$ is directly proportional to η giving

$$\frac{\Delta\eta(o)}{\Delta\eta(\phi)} - 1 = \tau_o K_\Delta \phi \qquad (17)$$

where K_Δ is the $\Delta\eta$ damage constant.

Combining equations (11) and (17) gives the relationship for power reduction at a constant current above threshold, that is $I - I_{th} = \text{const}$:

$$\frac{P(o)}{P(\phi)} - 1 = \tau_o K_\rho \phi \qquad (18)$$

where K_p is the power damage constant.

The model for radiation damage presented here is very simple. The basic assumption is that radiative lifetime increases linearly with respect to total lifetime when the material is exposed to a flux of fast neutrons. This results in a linear increase in threshold current and a linear decrease in power at a constant current above threshold. Although the model is simple, it has been used successfully to explain results in other studies such as those of Southward and Barnes.

CHAPTER III

EXPERIMENTAL EQUIPMENT AND PROCEDURES

Laser Diodes

The devices used for this study were manufactured by RCA and Laser Diode Laboratories, Inc. and supplied by the Air Force Weapons Lab. Both types of diodes are designed for continuous infra-red emission at room temperature. In both types the heterostructure is grown by liquid phase epitaxy, and both use a stripe contact to limit the width of the active region. Although much information about the construction of the diodes is proprietary, some of the main differences can be presented.

The RCA LCW-10 consists of probably four regions (Ref 11:234) with an oxide-isolation stripe contact. The active region of n-type $Al_yGa_{1-y}As$ is sandwiched between two layers of $Al_xGa_{1-x}As$, one p-type and one n. The value of y (probably about 0.1) is smaller than the value of x (probably about 0.3) so that the band-gap in the recombination region is less than that in the adjoining regions. A highly doped p-type GaAs layer is grown next to the p-type (AlGa)As layer to provide a better ohmic contact with the metallic stripe.

In the RCA diode, the contact stripe is formed by depositing a layer of insulating SiO_2 on the surface of the p^+ region. A 13 micron wide stripe is removed along the desired active area. The individual devices are made from the wafer by cleaving the wafer into slivers, and then sawing the slivers into sections. The cleaved ends of the device form the reflecting surfaces of a Fabry-Perot lasing cavity. The sawed edges have low reflectivity, thus they suppress horizontal modes in

the cavity.

After the individual diodes are formed, the laser is passivated, that is, the end facets of the laser are coated with a dielectric material to reduce the possibility of catastrophic degradation due to facet damage. The p side of the device is then indium-soldered to a copper heatsink with the SiO_2 insulating all but the stripe region.

The Laser Diode Laboratories LCW-10 is manufactured in much the same way with a few important differences. The aluminum concentration in the active region is slightly lower than that for RCA diodes, resulting in a shorter wavelength of emission. This region is also p-type rather than n-type as in the RCA devices. The sandwich layers contain a slightly higher concentration of aluminum (x=0.35) than the RCA diodes which may give better confinement of the active region. Also, there are two additional layers in the LCW-10, both n-type. The substrate is grown with a very low dislocation density ($1000/cm^2$) by the gradient-freeze technique. Onto this layer is grown a layer of n-type GaAs designed to terminate dislocation networks or substrate surface imperfections. These two layers greatly reduce the possibility of gradual degradation of the device caused by dislocation migration into the active region (Ref 7:4).

Additional precaution against defect formation is taken by using a monolithic stripe. Instead of etching a stripe in a deposited layer of an oxide insulator, a layer of n-type GaAs is deposited and then etched to form the 15 micron wide stripe. This n layer forms a reverse biased p-n junction which is nonconducting except in the stripe region where the n-type material has been removed. This method is

simple, it reduces the danger of forming lattice defects near the surface of the pellet, and reduces the stress on the surface of the chip. Additionally, thermal conduction from the laser to the heat sink is better because the oxide layer, which is a poor thermal conductor, is not presented (Ref 7:6-7).

Irradiation Facilities and Procedures

The source of neutrons used for irradiation of the laser diode samples was the Ohio State University nuclear reactor. It is a swimming pool reactor with a maximum power level of 10 kW. The core of the reactor consists of a 5-by-5 array of 20 fuel elements, 4 control rod elements, and a central irradiation facility (CIF). The fuel elements are standard 10 plate elements of U-Al alloy clad with aluminum. The enrichment is 93% U-235 (Ref 15).

Irradiations for this experiment were performed in the central irradiation facility of the reactor. This facility is a 1-1/2 inch diameter aluminum pipe located in the core at matrix position (3,3). The inside of the pipe is dry and samples may be lowered by string to the geometric center of the core. The unperturbed neutron flux in the CIF with the reactor operating at 10kW is 3.97×10^{11} n/cm^2-sec, of which 50% are thermal neutrons (E less than 4.75×10^{-7} MeV), 50% are epi-cadmium neutrons (E greater than $4.75\ 10^{-7}$ MeV), and 21% are fast neutrons (E greater than 0.5 MeV) (Ref Ohio State Handout on reactor fluxes). About 5% of the total dose at 10kW is due to gamma radiation. This is a dose of about 6×10^5 rad/hr which is much less than the gamma dose given to the diodes in Ackermann's work (Ref 1:37).

For this experiment, each sample was irradiated inside a 2 inch by 3/4 inch cylindrical plastic vial lined with 0.040 inch thick cadmium to absorb thermal neutrons. The liner consisted of a disc in the bottom of the vial, a 1 inch high cylinder, and a removable top. Since the end caps were not formed to overlap the cylinder, the liner was inspected visually before each irradiation to assure that there were no gaps.

The sample was placed inside the liner along with a nickel wire for monitoring the flux. No attempt was made to position the wire or the laser diode at a certain spot inside the liner. After the sample and wire were in place, the plastic vial was put in a basket and lowered by string into the core. A knot in the string was used to mark the distance from the top of the CIF pipe to the center of the core. Timing for the irradiation begun when the sample arrived at the core center if the reactor was already at full power when the sample was inserted, or, when full power (10kW) was reached if the sample was inserted before reactor startup. Timing was ended when the sample was removed from the core or when the reactor was shut down.

After the vial was removed from the reactor, the sample was removed and monitored for gamma and beta activity before its operating characteristics were tested. The flux monitoring wire was analyzed with a GeLi detector and a Canberra 4096 channel analyzer. A minicomputer program gave the activity of the Co-58 directly from the data in the analyzer. The 810keV photopeak of Co-58 was used to determine the activity of the wire.

Two diodes were irradiated at liquid nitrogen temperature. For this experiment, a cadmium liner was placed inside a polystyrene container. After the diode and flux wire were in place, the container was filled with liquid nitrogen and lowered into the CIF. After five minutes of irradiation, the container was removed and the diode was dumped into a cup of liquid nitrogen and carried to the experimental area where its operating characteristics were measured. The diode was not out of the liquid nitrogen more than a few seconds during transfer to the testing apparatus. After the first set of data was taken, the diode was allowed to warm to room temperature. It was then recooled and the measurements were repeated to determine if any annealing of defects had occurred.

Measurement of Laser Diode Characteristics

All laser diode characteristics were measured with the diode immersed in liquid nitrogen except for some preliminary measurements that were taken at room temperature. Liquid nitrogen was used because of the difficulty of maintaining a constant temperature when the diode was operated in air. Although the temperature of the laser diode was not monitored, heat generated during operation of the device was assumed to be dissipated by the liquid nitrogen.

Power output of the devices was measured with an EG&G 550 multi-probe with the flat filter installed. Because the sensitive area of the detector subtends only a fraction of the laser beam, relative power measurements were taken. To minimize the effects of errors in the alignment of the lasers, a piece of opalized glass was placed

against the outside wall of the dewar as depicted in figure 4. This dispersed the beam so that the position of the detector in the beam was not as critical. Under these conditions, measurements of power output versus input current were reproducible with less than 10% deviation in power at a constant current.

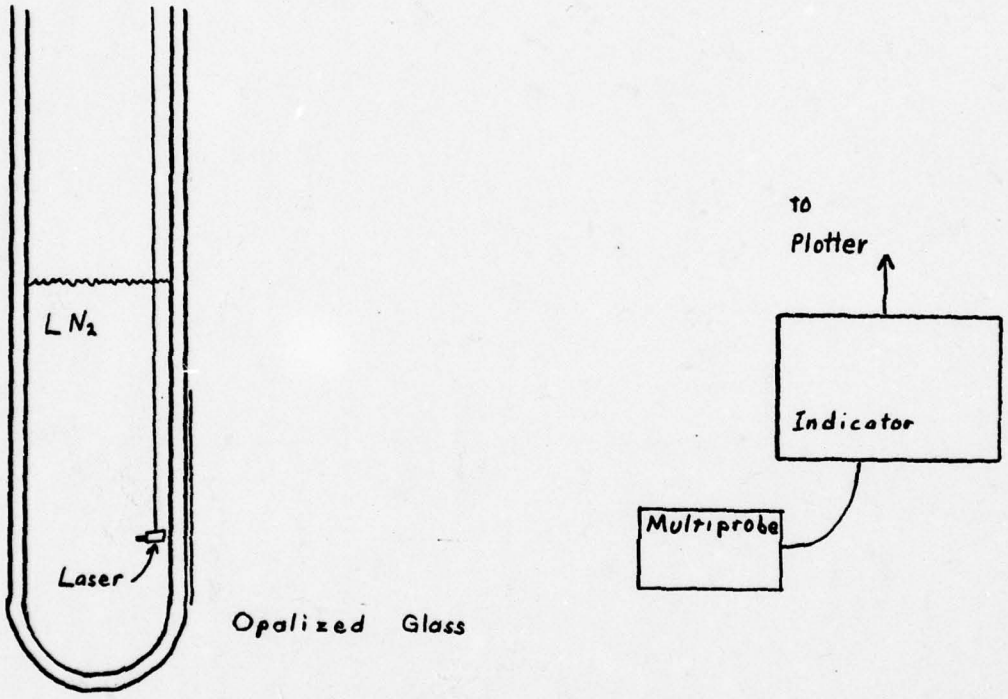

Figure 4

Apparatus for Measuring Power Output

The output of the multiprobe was connected through an EG&G 450-1 indicator to the y-axis of a Moseley Autograf Model 7001A x-y plotter. The x-axis of the plotter recorded the voltage drop across a 50-ohm resistor in series with the laser diode (see figure 5). The x-axis was calibrated so that its reading corresponded to the reading of the ammeter in series with the diode.

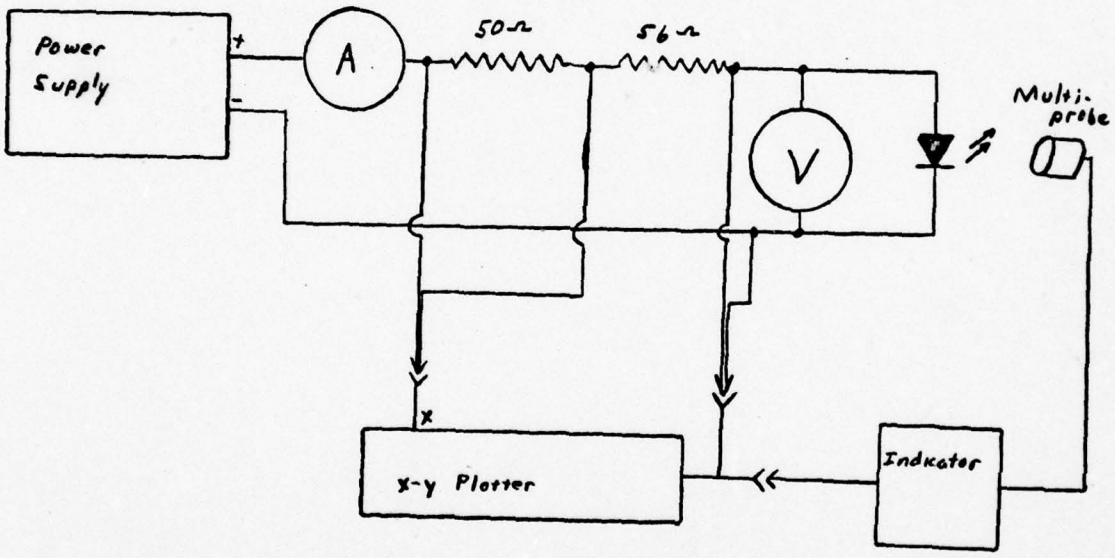

Figure 5

Circuit for Measuring Power and Voltage

Current versus bias voltage plots were made by disconnecting the radiometer output from the y-axis and connecting the input leads of the laser diode. The current was then increased to the maximum allowed and returned to zero.

The other measurement made for diodes that were irradiated was the spectral output. A Jarrell Ash 0.25 meter Ebert monochrometer with a motor drive was used to measure the spectra of the laser diodes at different operating voltages. The output of a silicon photovoltaic detector and amplifier mounted at the exit slit was connected to the x-axis of the plotter and the y-axis was set to sweep. The sweep was started at a known wavelength and the sweep rate was known, so the wavelength of the peaks could be determined. Additionally, the spectrum of a krypton lamp was superimposed on the laser spectrum when possible.

Voltage and current measurements were made by Honeywell Digitest model 333 multimeters. The power supply was one side of a Trygon Dual Lab Power Supply, model DL 40-1. Increases and decreases in bias current were made by manually increasing the power supply voltage.

CHAPTER IV

RESULTS

Neutron Flux Measurements

Although the values for the neutron flux published by the Ohio State University Nuclear Reactor Laboratory (NRL) are believed to be correct, nickel flux-monitoring wires were irradiated with each sample. The flux was calculated using the relationship

$$A_o = N\sigma\phi(1-e^{-\lambda t}) \tag{19}$$

or, for $t << t_{1/2}$

$$\phi = \frac{A_o}{N \sigma \lambda t} \tag{20}$$

where ϕ is the flux in neutrons per square centimeter per second, A_o A_o is the activity of Cobalt-58 in the flux wire in disintregrations per second, N is the number of atoms of nickel-58 before irradiation, σ is the cross section for the (n,p) reaction of nickel-58 in the reactor, λ is the decay constant for Co-58, and τ is the irradiation time.

The flux calculated from the activities of the wires was consistently higher than the value of 3.97×10^{11} n/cm^2-sec supplied by NRL. The wires were used more than once because of the long half-life of Co-58; however, due to the errors that accumulated during successive countings, only the first run for each wire was used. The fluxes

calculated from the first runs ranged from 5.97 x 10^{11} n/cm^2-sec to 1.03 x 10^{12} n/cm^2-sec, and averaged 7.78 x 10^{11} n/cm^2-sec with an average statistical uncertainty of 3.3%. Because of this discrepancy, an aluminum wire was used for one of the irradiations. Results from the (n, α) reaction gave a flux of 9.24 x 10^{11} n/cm^2-sec, and from the (N,p) reaction gave 7.79 x 10^{11} n/cm^2-sec. These results confirmed the values obtained with the nickel wires. The best estimate for the flux using calculations from the monitoring wires is 7.94 x 10^{11} n/cm^2-sec, exactly twice the value supplied by NRL.

Reasons for this discrepancy include errors in the calculation of the crossections by NRL, or a perturbation of the neutron flux by the cadmium lining of the sample container. The reactivity effect of the cadmium was -0.24%. The effect of this negative reactivity was to decrease the neutron flux, requiring control rods to be pulled farther out of the core to maintain full power. Since the reactor is controlled by monitoring the flux from a point outside the core, the flux at the center of the core may have been increased by a factor of almost two, while the flux at the edge of the core decreased sufficiently to keep the total power at 10 kW.

Further experiments are being done to resolve this uncertainty, but, until more is known, values of flux obtained by analyzing the wires will be used. Values reported in this paper are based on a flux of 1.68 x 10^{11} n/cm^2-sec which is the fast neutron flux (E greater than 0.5 MeV) obtained from the calculations.

Irradiation Effects on Laser Diodes

The performance of the laser diodes was significantly degraded by exposure to the neutron flux. The first diode irradiated, an RCA C30127, #70, received a fast neutron fluence of 1.81×10^{15} neutrons per square centimeter. After this irradiation, the diode did not perform as a laser, so the dose for the next diode was reduced by a factor of ten.

The other diodes all showed continued degradation with each irradiation. A typical result is shown in Figure 6, the relative power output of RCA diode number 550 as a function of forward current at several fluences. One evident effect of irradiation is an increase in threshold current. In addition, there is a decrease in the differential quantum efficiency.

The increase in threshold current for the four diodes that received step irradiations is shown in Figure 7. Threshold current was determined by extrapolating the first increase in the power versus current curve back to the current axis. The point of intersection was taken to be I_{th}. The unirradiated threshold current for Laser Diode Labs devices was about twice that of the RCA diodes, and the relative increase in threshold current of the Laser Diode Labs diodes was about twice as high, also.

The increases are linear up to about 10^{15} n/cm^2, supporting the model developed in Chapter II. Above this value, the threshold current is higher than that predicted by the linear model. There are several possibilities for the cause of this deviation. The most likely is the imprecision of measuring the threshold current. There

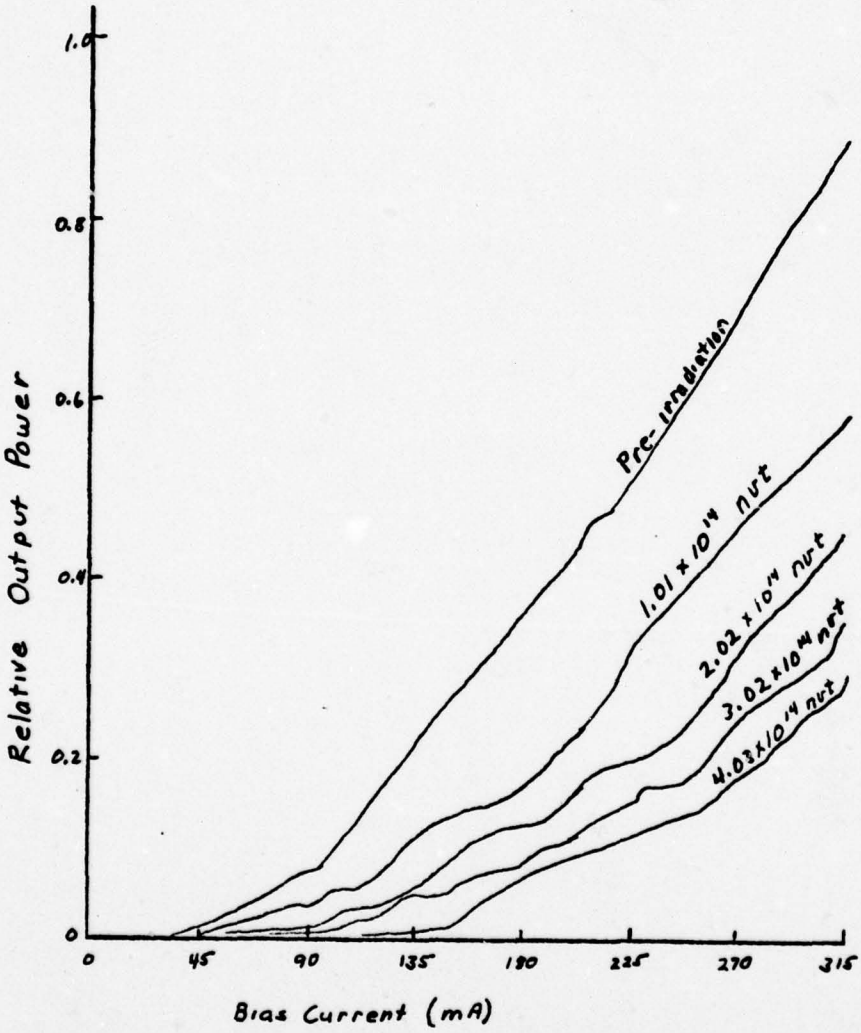

Figure 6

Power vs. Current of RCA #550 at Several Fluences

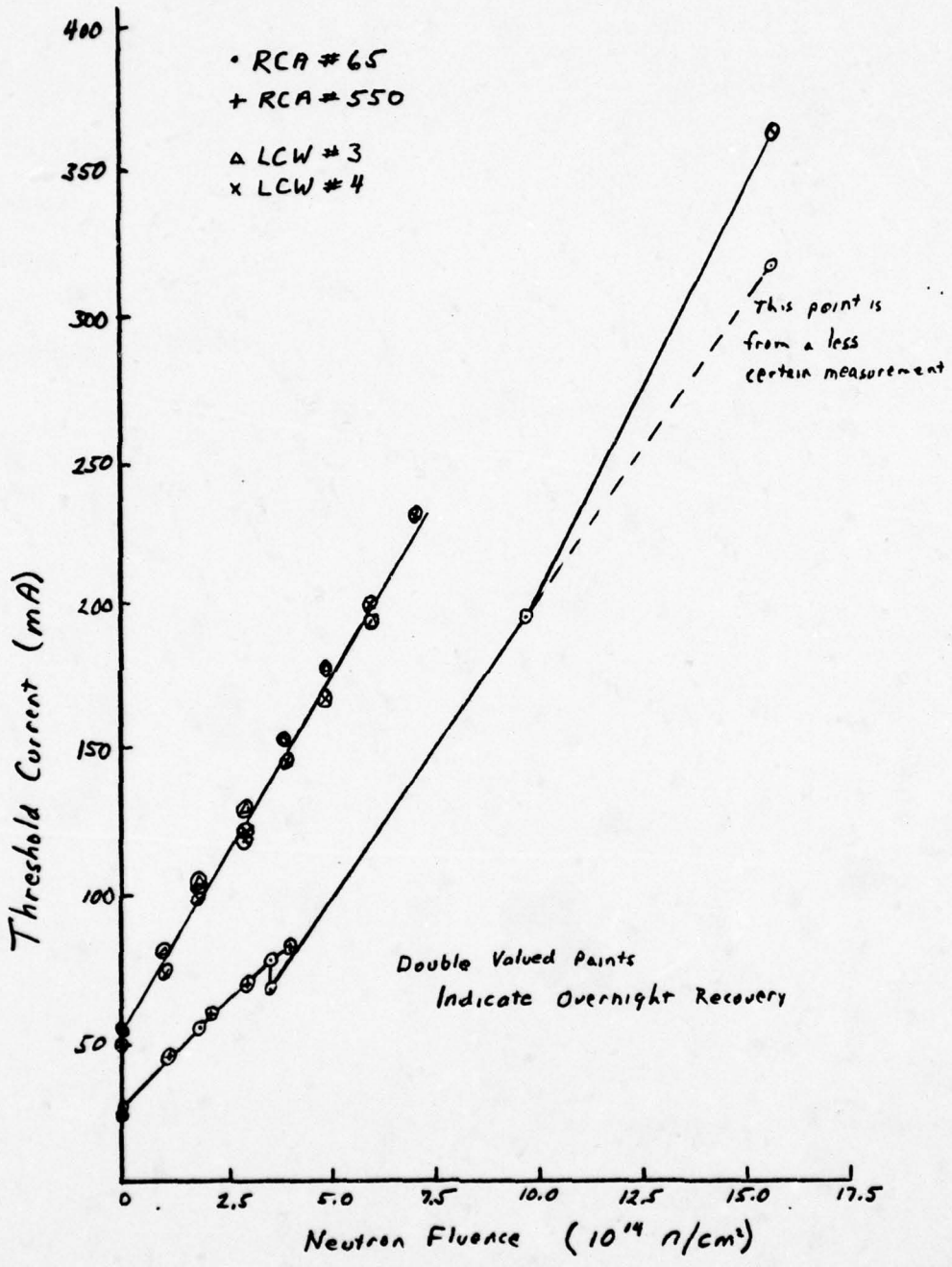

Figure 7

Increase in Threshold Current vs. Neutron Fluence

is only one point above 10^{15} n/cm^2. Although the plots of output versus input current for this fluence show a definite increase in output that extrapolates back to 365 mA, there is a short region of the curve that extropolates to 310 mA, close to the value predicted by the linear model. Another possibility is that the increase in threshold current is actually greater at higher fluences due to an effect other than the formation of nonradiative centers. This could include an increase in the absorption coefficient in the active region or in a loss of some of the wave guiding ability of the heterojunction structure. For the purposes of this paper, the reason for the non-linearity in this region, if it exists, is not important because an increase in threshold current of this amount at 77°K would be an increase to well above the maximum allowed current for the devices at room temperature.

If all four curves for increases in I_{th} with increasing fluence are assumed to be linear, the damage factor, $\tau_o K_I$, from equation (16) can be calculated. These factors appear in Table I. The values of $\tau_o K_I$ are computed by adding the over-night recovery amount to all measurements taken the next day. The last value for RCA number 65 is not included in the calculation because of its uncertainty. Therefore, the values for $\tau_o K_I$ in the table should be considered useful only for values of ϕ below about 10^{15} n/cm^2.

Table I

$\tau_o K_I$			
RCA #65	5.93×10^{-15} cm^2	LDL #3	4.53×10^{-15} cm^2
RCA #550	5.13×10^{-15} cm^2	LDL #4	5.22×10^{-15} cm^2

The decrease in differential quantum efficiency for each of the four diodes tested in this experimental phase was much more difficult to measure because of the irregular behavior of the output power versus input current curves. Figure 8 is an example of the large discontinuity encountered in diode number 65. Although the other diodes behaved less erratically, all exhibited some sort of kink or discontinuity which generally increased in severity as the fluence increased.

The differential quantum efficiency was measured in two ways. First, the slope of the P versus I curve at $(I - I_{th})$ = const was measured graphically by dividing the change in power over a small region by the change in current over the same region. This technique proved to be less than optimum because of the many changes in $\Delta\eta$. The second method was an attempt to find the average $\Delta\eta$ over the entire region above threshold. A straight line was drawn using the least squares regression technique, that best approximated the P versus $(I - I_{th})$ line, and the slope of this line was taken to be $\Delta\eta$. Since the purpose of this study is to be able to predict the output power of a device at a given neutron fluence, this method was thought to be the most useful. The results of this measurement appear in Figure 9. Although the lines in Figure 9 are not straight as predicted; the varied deviations from linearity do not suggest any other trend. The slopes of the straight line approximations to the data in Figure 9 are the factors $\Delta\eta$ in equation (17) for each of the diodes. These values are tabulated in Table II.

The reduction of output power as a function of neutron fluence is closely related to the reduction in differential quantum efficiency.

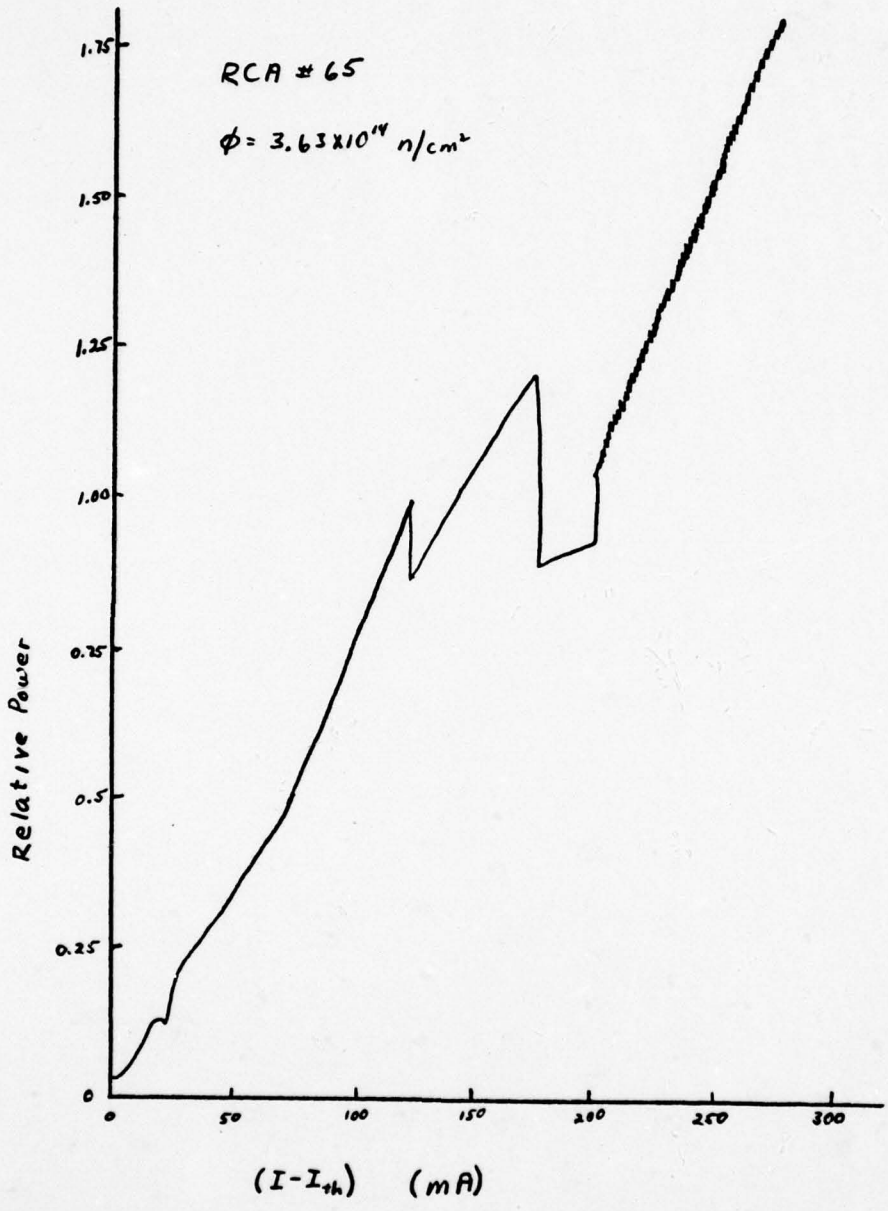

Figure 8

Power Versus (I-I_{th}) for RCA #65

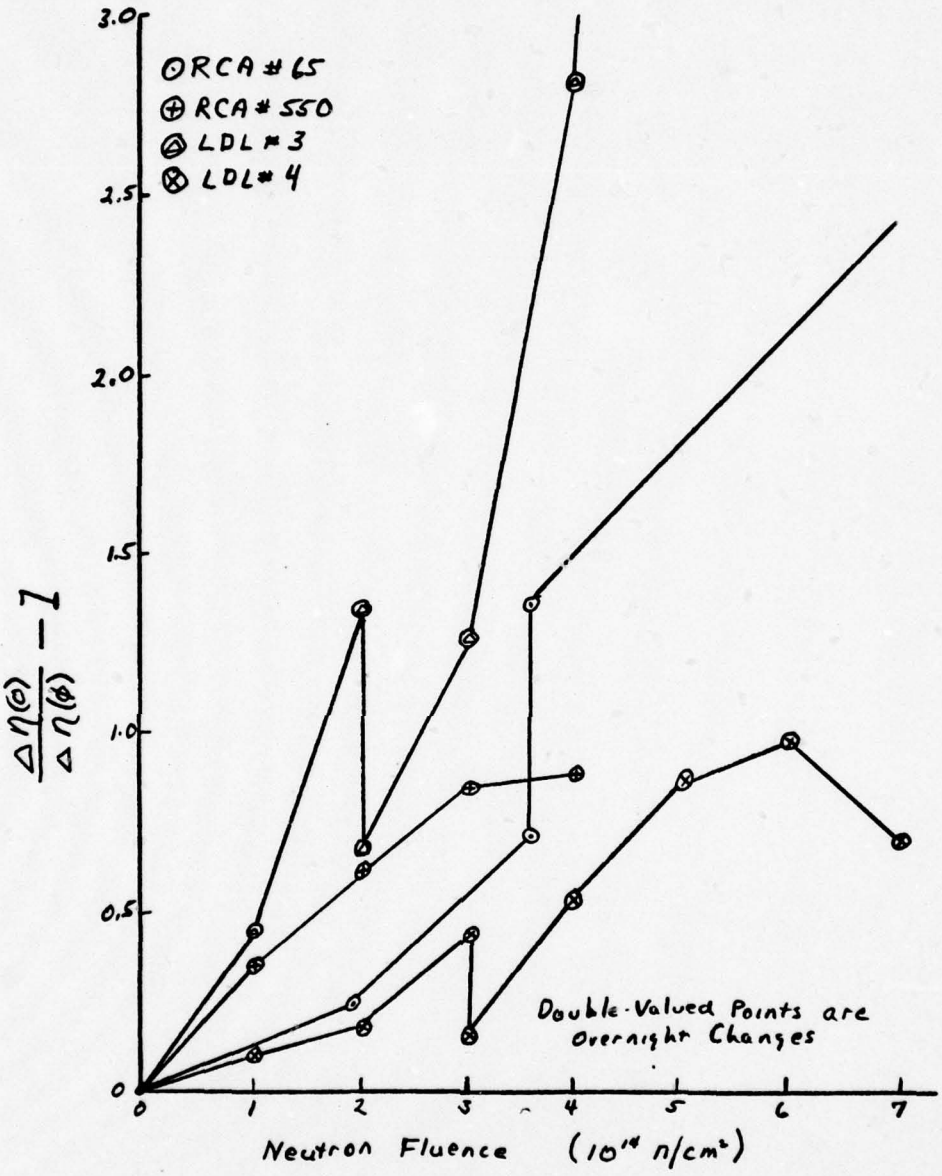

Figure 9

Change in Differential Quantum Efficiency
vs.
Neutron Fluence

Table II

	$\tau_o K_\Delta$		
RCA #65	2.72×10^{-15} cm^2	LDL #3	8.43×10^{-15} cm^2
RCA #550	2.23×10^{-15} cm^2	LDL #4	1.89×10^{-15} cm^2

The relative output power of each of the four diodes tested is displayed in Figure 10. These values are arbitrary power units taken at 100 mA above threshold for each device. These values are erratic and appear to follow no pattern for two of the diodes, LDL #4 and RCA #65. The other two, LDL #3 and RCA #550 show an approximately linear decrease in power with increasing neutron fluence. The erratic behavior of the first two curves mentioned is probably due to anomalies in the P versus I curve at $I-I_{th} = 100$ mA. Since two of the diodes show a linear decrease, a linear function for all four may be assumed. The values of $\tau_o K_p$ from equation 18 were found by least squares linear regression to $\frac{P(o)}{P(\phi)} - 1$ points with a correction for overnight recovery as described for differential quantum efficiency. The values for $\tau_o K_p$ are presented in Table III.

Table III

	$\tau_o K_p$		
RCA #65	5.19×10^{-16} cm^2	LDL #3	9.00×10^{-15} cm^2
RCA #550	4.05×10^{-15} cm^2	LDL #4	-7.79×10^{-17} cm^2

The results discussed to this point are useful primarily for verifying the model derived in Chapter II. For practical purposes, the

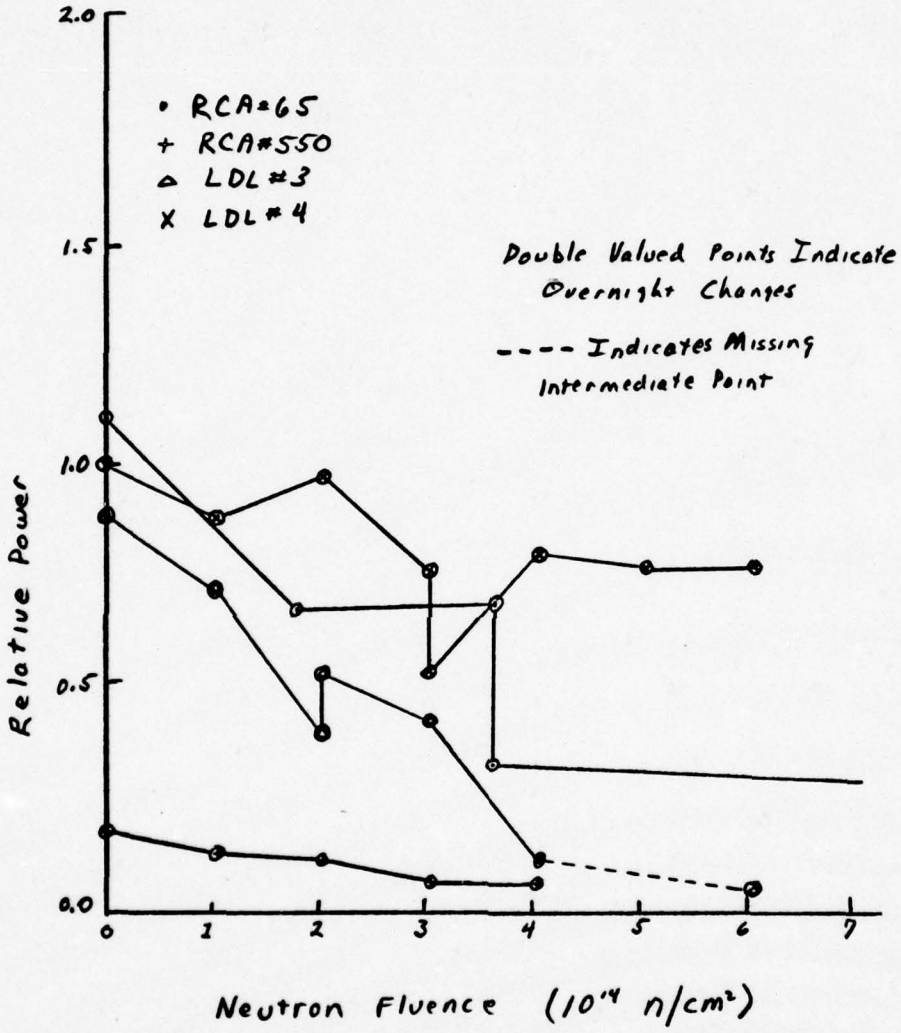

Figure 10

Relative Power at 100 mA Above Threshold
vs
Neutron Fluence

effect of the neutron fluence on the relative output at a constant current or constant voltage is important. From the damage model, the relative output at constant current as a function of ϕ should be

$$P(\phi) = \Delta n(\phi)[I - I_{th}(\phi)] \qquad (21)$$

Because of the anomalies in the power output curves, this equation will not predict the power output exactly. The measured relative power at 200 mA for each diode is plotted in Figure 11. As seen, the output power at constant current decreases as the inverse square of the neutron fluence. No single factor was derived for predicting the power output at a constant current because it can be predicted using damage factors already derived along with equation (21).

In addition to measurements of power versus current, voltage versus current measurements were taken. A typical plot of V versus I is shown in Figure 12. In this experiment, there was no appreciable change in the voltage required to produce a given current, indicating that either the effect of a neutron fluence on the diode resistance was very small, or that more than one effect was taking place and the effects nearly canceled each other.

From previous studies, at least two effects on V versus I curves would be expected when a GaAs semiconductor is irradiated with neutrons. Aukerman (Ref 2) reported an increase in resistivity of the GaAs material with neutron irradiation. Southward reported an increase in current at constant voltage for irradiated GaAs diffused laser diodes

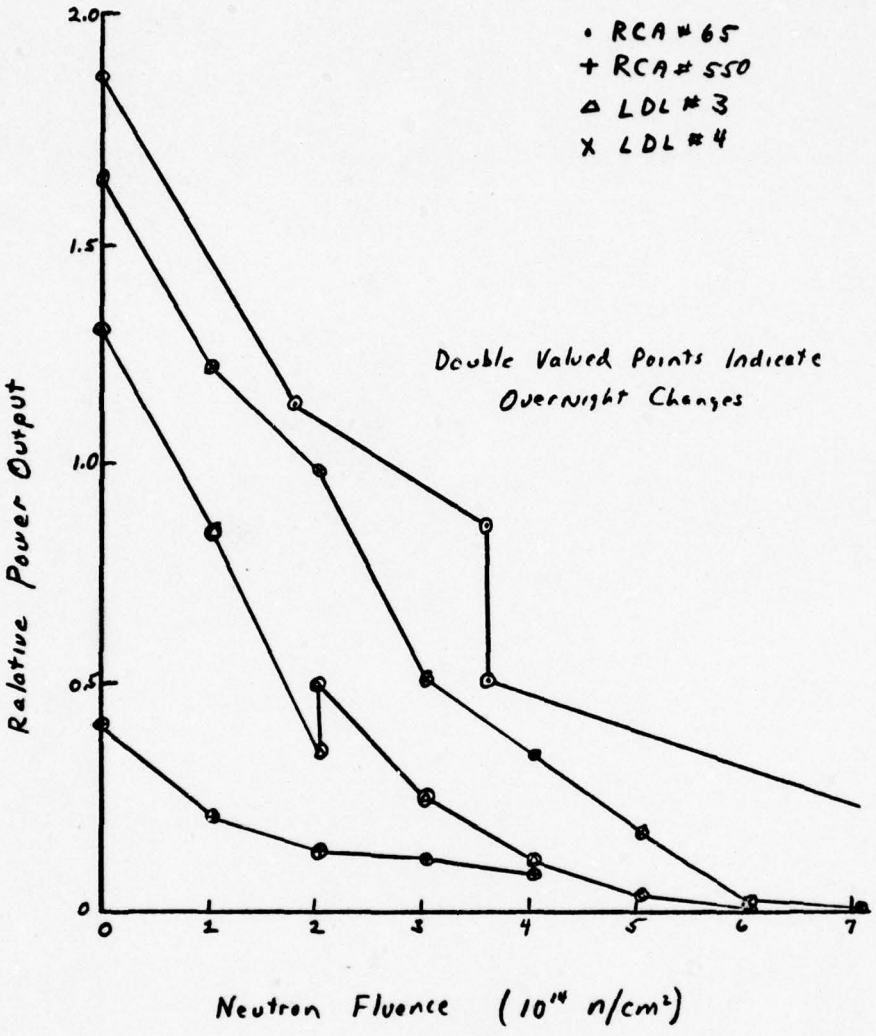

Figure 11

Relative Power Output at 200 mA
vs
Neutron Fluence

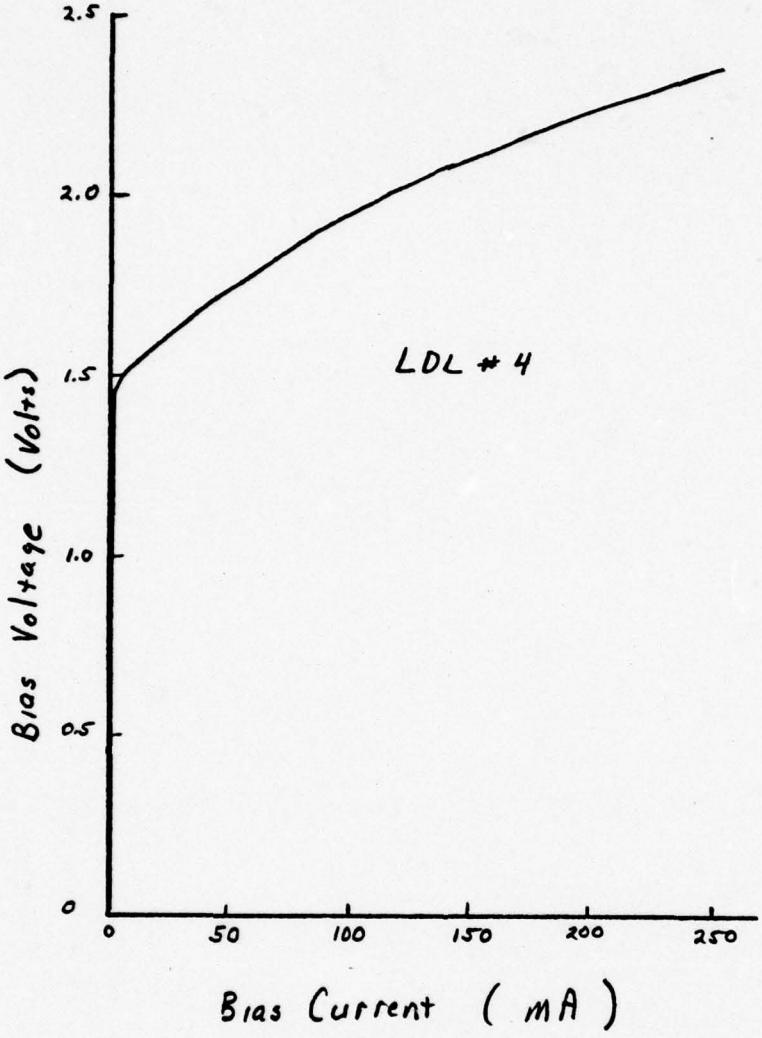

Figure 12

Bias Voltage
vs
Forward Current

(Ref 19:5). The increased current from a decreased carrier lifetime coupled with increased IR losses could account for the lack of significant changes in this study. If the change in I versus V was very small, it would not be detectable with the equipment used due to the slope of the I versus V line in the operating region. For this report, it will be assumed that no change in the voltage required for a given current occurred.

The last data taken were spectral measurements of the laser output. After irradiation, there was no significant change in the peak wavelength for lasing, indicating that the neutron fluence did not affect the energy bandgap for the lasing transition. There was, however, a shift in peak wavelength with increasing voltage indicating that the tunneling mechanism described in Chapter II is taking place. Additionally, some diodes showed a tendency to lase at two wavelengths separated by about 3 nm to 4 nm. This suggests that there are two cavities for lasing instead of the one cavity for which the lasers are designed. The different wavelengths become dominant at different bias currents, but no constant relationship could be derived.

The results of irradiations at liquid nitrogen temperatures were inconclusive. Because the container could only hold enough liquid nitrogen for a five-minute irradiation, the reduction in power was only slightly more than the reproducibility limits of the measurements (about 10%). One diode showed no change in operating characteristics after being warmed to room temperature. The other showed a slight, but insignificant increase in power output versus current.

CHAPTER V

DISCUSSION AND RECOMMENDATIONS

Discussion of Results

The results of this work show that AlGaAs, double heterojunction, stripe geometry laser diodes behave much like diffused GaAs lasers when exposed to a flux of fast neutrons. The linear nature of the degradation of threshold current, differential quantum efficiency, and output power at a constant current above threshold suggest that the simple model developed in Chapter II is probably adequate.

It must be remembered that the damage factors for laser operation were derived from measurements taken at 77° K and not at room temperature. The purpose of immersing the diodes in liquid nitrogen was to provide more control over the operating temperature of the diode. When applying these data to devices operating at room temperature, the fact that pre-irradiation threshold current is much higher must be taken into account. Moreover, the factor $\tau_o K_I$ would be expected to be higher because τ_o is larger at room temperature than at 77° K. The temperature dependence of $\tau_o K_I$ is demonstrated in the results of Southward's study (Ref 19:217). The relationships suggest that I+L will approach maximum allowable current at much smaller fluences at room temperature than at 77° K. An estimate of the threshold current versus neutron fluence at room temperature is given in Figure 13. Additional study of the operation of these diodes at room temperature must be done before their suitability for use in Air Force systems can be determined.

An interesting and unexpected result of the measurements of

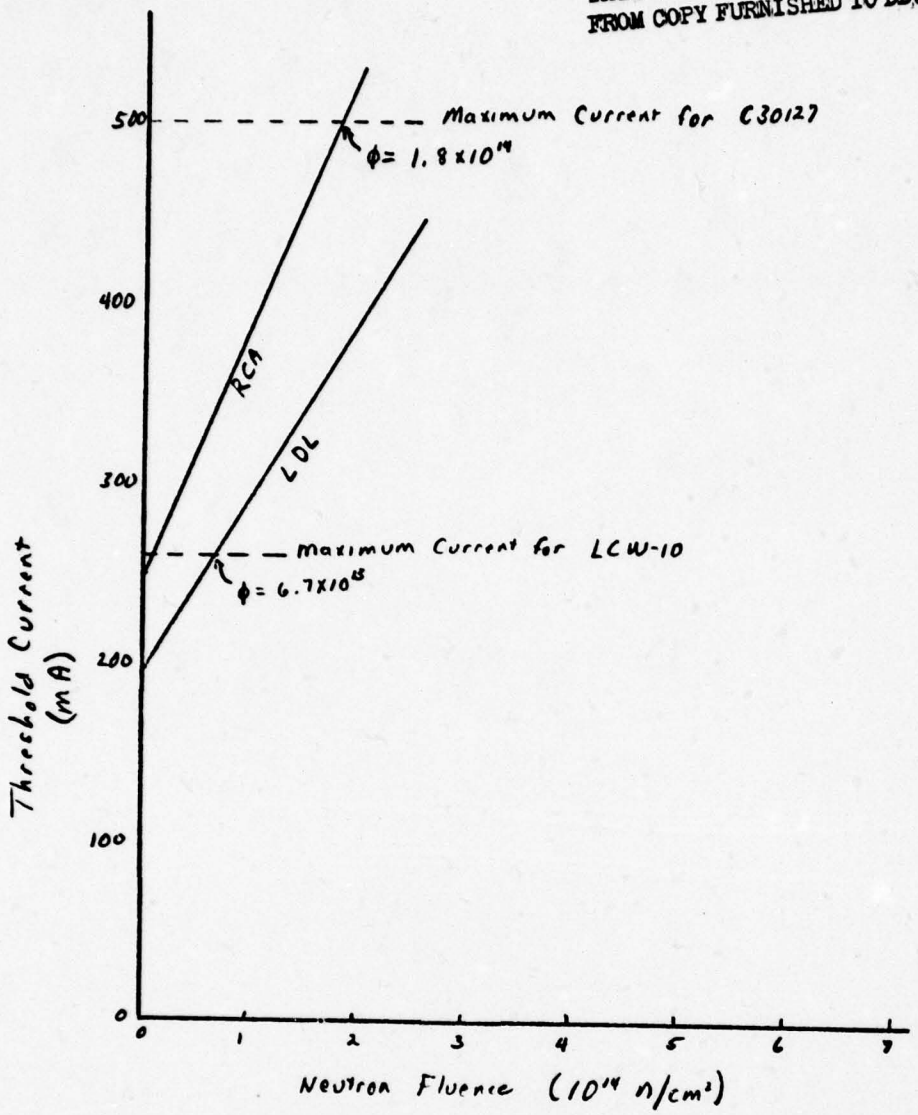

Figure 13

Estimated Increase in Threshold Current
vs
Neutron Fluence
at Room Temperature

power versus current was the significant departure from linearity. Kinks in power output versus current curves have been observed before (Refs 6,10,18) and explained in a number of ways. Kobayashi (Ref 10:659) suggests that the horizontal modes of the laser are unstable and that the number and intensity of these modes changes with the pumping level. As the pumping level is increased, the confinement of the horizontal mode is decreased because the threshold gain region extends farther laterally. This causes the horizontal component of the beam to extend farther away from the center of the device where there is more loss. The result is an increase in the total apparent cavity loss, α , and a reduction in the differential quantum efficiency. Thus, a kink or nonlinearity appears in the output versus current curve of the diode.

Risch and others (Ref 18) have used an external cavity to study the nonlinearities in AlGaAs lasers. They concluded that the internal quantum efficiency of their devices was near 100% and was independent of the current density. The anomalies appeared to be related to the ratio between stimulated and spontaneous emission rates (Ref 18:695).

The most likely hypothesis in light of the results of the current study is proposed by Campos and others (Ref 6). The fact that the near field transmission pattern changes in the kink region of the laser output led Campos and his colleagues to believe that the anomalies are due to competition between two cavities within the device. They propose that at low currents, the gain losses are high and the area of least loss determines the lasing cavity. The longitudinal axis of the cavity may be angularly displaced several degrees from the perpen-

dicular to the cleaved ends of the diode. As the current density is increased, the gain throughout the active region becomes more uniform and the mirror losses determine the location of the lasing cavity. Since the factor R is different for the two cavities, the differential quantum efficiency will change when the diode changes cavities and a nonlinearity or kink will appear in the P versus I curve.

Some devices used in the current study showed a tendency for the beam to change direction in the far field as the current was increased. Sometimes the beam would change back to the original direction as current was increased more, and continue to jump back and forth as the current was further increased. The P versus I curve of these devices showed several nonlinearities and some discontinuities. No one else has reported discontinuities in the P versus I curves of laser diodes, and the cause for their appearance is not known. Possibly, the abrupt change of laser cavities as the current is changed also causes the internal quantum efficiency (for stimulated emission) and consequently the power output of the device to change. Another possibility is that the most intense portion of the beam missed the detector when the laser cavity changed, even with a diffuser near the window of the diode.

Whatever the cause of these anomalies, they are undesirable for communications systems. When the laser is modulated by varying the input current, the output should be linear and at least be single valued for a given current. Devices showing discontinuous behavior such as RCA #65 in this study would be likely to transmit false information because a discontinuity could be interpreted as a pulse.

Although the anomalies disappeared after exposure to higher neutron fluences, moderate fluences caused the discontinuities to become more prominent. If the cavity competition model for the anomalies is correct, the reduction of η_i by irradiation may cause the inhomogeniety to be enhanced, thus intensifying the nonlinear effects.

Another factor which must be considered when using the damage constants obtained in this study is the source of neutrons. According to Lambert and others (Ref 13), the type and dose rate of radiation is important as well as total dose. Although the energy spectrum of the neutrons used for irradiation in this experiment may be similar to the air moderated spectrum from a nuclear weapon, there are differences that will give some effect. As the energy of the neutrons increases, an increase in the damage factor would be anticipated.

The dose rate for this experiment was considerably less than that expected from a nuclear blast. Lambert found that neutrons from a high flux accelerator inflicted five times as much damage in semiconductors as the same total dose from a nuclear reactor (Ref 13:297).

Recommendations

Before using the AlGaAs diode lasers in USAF weapons systems, more studies should be done on radiation effects. The effects of a neutron fluence on room temperature operation should be studied using a high dose rate source. This would give a better estimate of actual performance after a nuclear blast. In addition to the studies of power output, studies of rise time and time delays should be completed.

The data in this experiment were all taken after irradiation was complete, and flux induced charge carriers had recombined. An

experiment to determine the transient effects of radiation on the lasers must be done because flux induced currents may damage the devices or associated circuitry significantly.

Bibliography

1. Ackermann, H. Effects of Gamma Radiation on Gallium-Arsenide Lasers. Unpublished Thesis. Wright-Patterson Air Force Base, Ohio: Air Force Institute of Technology, December 1977.

2. Aukerman, P. W., et al. "Radiation Effects in GaAs." Journal of Applied Physics, 34: 3590-3599 (December 1963).

3. Barnes, C. E. "Neutron Damage in Epitaxial GaAs Laser Diodes." Journal of Applied Physics, 42: 1941-1949 (April 1971).

4. Barnes, C. E. "Neutron Damage in GaAs Laser Diodes: At and Above Laser Threshold." IEEE Transactions of Nuclear Science, NS-19: 382-385 (December 1972).

5. Bolz, R. E., and G. L. Tuve. Handbook of Tables for Applied Engineering Science, (Second Edition). Cleveland, Ohio: CRC Press, 1973.

6. Campos, M. D., et al. "Cavity Competition in Anomalous Emission Intensity in Double-Heterostructure (DH) Lasers." IEEE Journal of Quantum Electronics, QE-13: 687-691 (August 1977).

7. Grill, R. B., et al. Injection Laser Sources for Fiber Optic Communications. Metuchen, New Jersey: Laser Diode Laboratories, Inc.

8. Hayashi, I., et al. "Junction Lasers Which Operate Continuously at Room Temperature." Applied Physics Letters, 17: 109-111 (1 August 1970).

9. Hemenway, C. L., et al. Physical Electronics (Second Edition). New York: John Wiley and Sons, Inc., 1967.

10. Kobayashi, K. "Unstable Horizontal Transverse Modes and Their Stabilization With a New Stripe Structure," IEEE Journal of Quantum Electronics, QE-13: 659-661 (August 1977).

11. Kressel, H., and I. Ladany. "Reliability Aspects and Facet Damage in High-Power Emission from (AlGa)As CW Laser Diodes at Room Temperature." (RCA Review, 36: 230-239 (June 1975.

12. Kressel, H. "Semiconduction Lasers" in Lasers, Vol. 3, edited by A. K. Leving and A. J. Demaria. New York: Marcel Dekker, Inc., 1971.

Bibliography (cont'd)

13. Lambert, K. P., et al. "A Comparison of the Radiation Damage of Electronic Components Irradiated in Different Radiation Fields." Nuclear Instruments and Methods, 130: 291-300 (December 1975).

14. Lederer, M. C., et al. Table of Isotopes (Sixth Edition). New York: John Wiley and Sons, 1967.

15. Ohio State University. Reactor Description and Hazards Summary Report for the Ohio State University Reactor. March 1965.

16. O'Shea, D. C., et al. A Laser Textbook. Georgia Institute of Technology, September 1975.

17. Rediker, R. H. "Semiconductor Lasers." Physics Today, 18: 42-50 (February 1965).

18. Risch, C. H., et al. "External-Cavity-Induced Nonlinearities in the Light Versus Current Characteristics of (Ga,Al) As Continuous Wave Diode Lasers." IEEE Journal of Quantum Electronics, QE 13: 692-696 (August 1977).

19. Southward, H. D., et al. Fast Neutron Effects on Diffused Gallium Arsenide Lasers. AFWL-TR-73-23. Kirtland Air Force Base, New Mexico: Air Force Weapons Laboratory, 1973. AD 912532

20. Sze, S. M. Physics of Semiconductor Devices. New York: Wiley-Interscience, 1969.

21. Taylor, D. Neutron Irradiation and Activation Analysis. Princeton, New Jersey: D. Van Nostrand and Company, Inc., 1964.

APPENDIX A

REQUEST FOR REACTOR OPERATION

The request for reactor operation includes a hazard analysis for the irradiated diodes. The data for calculating the activities cam from Lederer (Ref 14) and Taylor (Ref 21). Although the activity calculated for the diodes is high, the calculations are conservative. The actual exposure rate from irradiated diodes was about 500 mR/hr at 10 cm immediately after a 10-minute irradiation. The exposure rate quickly decayed to about 100 mR/hr.

The experimental apparatus was surrounded by a 4-inch wall of lead bricks to protect the experimenter from excessive exposure. The wall was erected as a consequence of the results of the hazard calculations, but probably was not needed since the time of exposure to the devices was short.

NRL — 1555

REQUEST FOR REACTOR OPERATION

THE OHIO STATE UNIVERSITY — NUCLEAR REACTOR LABORATORY
1298 KINNEAR ROAD / COLUMBUS, OHIO 43212 / PHONE (614) 422-6755

Date 13 October 1977

To: OPERATIONS SUPERVISOR

From: Dr. G. R. Hagee GRH (Initials)

Address: AF Institute of Technology (AFIT/ENP), WPAFB OH 45433

Phone: (513) 255-2012

Reactor requested for 27 Oct-16 Nov 19 77

Power level: 10 kW Facility desired: CIF

APPROVALS:

I ☐ II ☐ III ☐ IV ☐ V ☐ VI ☐ VII ☐ VIII ☐ IX ☐ X ☐

By _____ DATE _____

Performed: _____ Date _____ Logbook _____ Page _____

CHARGES:

Physics — DEPT. NAME — DEPT. NO.

NE 7.99 — COURSE OR PROJECT NO. — BUDGET ACCT. NO.

Grad Research — OTHER IDENTIFICATION

DURATION OF EXPERIMENT — $ _____/_____ CHARGE

The REQUEST should be written in four distinct, and titled, parts: (1) Purpose, (2) Description/Procedure, (3) Safety Analysis, and (4) References.

PURPOSE

Activate five CW laser diodes to determine neutron radiation damage.

DESCRIPTION/PROCEDURE

Student (Capt Walsh) will arrive at 1300 on 26 Oct 77 to prepare first laser diode for irradiation on 27 Oct 77. A five-hour irradiation and post irradiation monitoring will be completed by reactor personnel. The other four lasers (2 RCA, 2 Laser Diode Labs) will be irradiated for two 3-hour periods, one period on the morning of each of the following days:

Monday, 31 October

Tuesday, 1 November

Wednesday, 2 November

Monday, 7 November

Thursday, 10 November

Monday, 14 November

Tuesday, 15 November

Wednesday, 16 November

Capt Walsh will prepare each of the samples on the working day prior to irradiation. Reactor personnel will place the sample in the reactor, and Capt Walsh will perform tests on the laser's output after each irradiation. The tests will take approximately 3 hours to complete. Capt Walsh will be responsible for radiation protection from irradiated samples in the test area.

Equipment will be set up in the OSU reactor building in a designated area on 28 Oct 77, and will remain in place until termination of the experiment.

Samples to be irradiated are GaAlAs injection lasers weighing 2.06 grams. They are composed of copper, iron, nickel, manganese, cobalt, gold, gallium, arsenic, aluminum, and indium. Each sample will be cleaned thoroughly and placed in a right cylindrical shield of 40 mil cadmium(height=1 in, wt = 19.4 g). A nickel flux monitoring wire will be placed in the cylinder of cadmium and the assembly will be placed inside a 1" by 2" plastic vial with a snap top.

Irradiated samples will remain at OSU until the completion of the experiment when they will be transported back to WPAFB in containers provided by AFIT.

Post-irradiation analysis of flux monitoring wires will be performed on the GeLi detector at NRL.

SAFETY ANALYSIS

Reactivity effect: Cadmium cylinder 1" high with closed ends.

Assume 3" cylinder with open ends which gives effect of -0.32% per 18g of cadmium.[2]

$$\text{effect} = (-0.32\%) \times \frac{19.4\text{g}}{18\text{g}} = -0.34\%$$

Expected activities of principal isotopes in irradiated diodes:

Activities were calculated using thermal neutron cross sections and a neutron flux of 1.97×10^{11} neutrons per cm^2 per sedond (CIF epi-Cd)

Major Radionuclides from Laser Diode

Radio-nuclide	Half-life	Activity ntps (3-hr irradiation)	Activity ntps (6-hr irradiation)	$\Sigma f_i \times E(MeV)$
^{59}Ni	8×10^4y	6.15	12.1	no gamma
^{63}Ni	125y	715	1.43×10^3	no gamma
^{65}Ni	2.56h	6.60×10^6	9.53×10^6	0.565
^{60m}Co	10.47 min	6.43×10^9	6.43×10^9	4.56×10^{-3}
^{60}Co	5.24 y	5.83×10^6	1.16×10^7	2.51
^{56}Mn	2.576 h	3.82×10^9	5.52×10^9	1.68
^{55}Fe	2.60 y	1.80×10^4	3.61×10^4	no gamma

REQUEST FOR REACTOR OPERATION NRL — 1555

Date 13 October 1977

Radio-nuclide	Half-life	Activity (3-hr irradiation) ntps	Activity (6-hr irradiation) ntps	$\Sigma f_i \times E$ MeV
^{64}Cu	12.80 h	7.74×10^{8}	1.43×10^{9}	0.194
^{66}Cu	5.10 min	1.18×10^{9}	1.18×10^{9}	9.35×10^{-2}
^{198}Au	270 d	1.85×10^{6}	3.71×10^{6}	0.40
^{114m}In	50 d	2.12×10^{5}	4.23×10^{5}	7.97×10^{-2}
^{114}In	72 sec	2.45×10^{8}	2.45×10^{8}	2.21×10^{-3}
^{116m}In	54 min	6.91×10^{9}	7.59×10^{9}	2.49
^{116}In	13 sec	3.99×10^{11}	3.99×10^{11}	1.70×10^{-2}
^{70}Ga	21.1 min	7.15×10^{7}	7.17×10^{7}	5.48×10^{-3}
^{72}Ga	14.3 hr	1.833×10^{7}	3.42×10^{7}	2.48
^{76}As	26.7 h	2.49×10^{7}	4.80×10^{7}	0.375
^{28}Al	2.27 min	2.84×10^{7}	2.84×10^{7}	1.78

Assume Exposure rate(R/hr)= 55.74 E(Mev) C(Ci)

a) Assume 1 one-MeV gamma per nt

Exposure rate = 631 R/hr @ 10 cm for 3-hr irradiation

= 635 R/hr @ 10 cm for 6-hr irradiation

b) Assume f_i x E gamma per nt

Exposure rate = 46.5 R/hr @ 10 cm for 3-hr irradiation

= 53.9 R/hr @ 10 cm for 6-hr irradiation

Expected activity of cadmium liner:

Radio-nuclide	Half-life	Activity ntps, 3hr	Activity ntpd, 6hr	$\Sigma f_i \times E$(MeV)
^{107}Cd	6.7 h	6.66×10^{7}	1.15×10^{8}	5.24×10^{-3}
^{111m}Cd	0.81 h	4.67×10^{8}	5.03×10^{8}	2.77×10^{-1}
^{113m}Cd	5.1 y	2.24×10^{4}	4.47×10^{4}	2.65×10^{-4}
^{115m}Cd	1032 h	1.66×10^{6}	3.31×10^{6}	3.09×10^{-2}
^{115}Cd	1272 h	1.48×10^{6}	2.96×10^{6}	3.61×10^{-1}

REQUEST FOR REACTOR OPERATION NRL — 1555

Date 13 Oct 77

Page 4 of 6

Exposure at 10 cm after 6 hours of irradiation is $\frac{55.74}{3.7 \times 10^{10}}$ (A) (f_i xE)

Exp. rate = 213 mR/hr @ 10 cm

Expected activity of 0.1 g of nickel wire:

Isotopes produced are ^{59}Ni, ^{63}Ni, and ^{65}Ni.(See page 2)

~~Exposure~~ Exposure rate (calculated as before) = 2.39 mR/hr @ 10 cm.

Experimenter will wear film badge and pocket dosimenters supplied by AFIT.

Activated samples will be packaged and transported in accordance with DOT regulations.[3] After completion of the experiments, they will be placed in a polyethelene capsule and then placed in a lead pig which will reduce the radiation level to less than 0.1 mR/m at the surface. These materials will be released under the USAF by-product material license No. 34-00472-02 submitted with previous request.[1]

REFERENCES

1. Request for Reactor Operation, 1 Sep 77, NRL 1548.

2. NRL 1087, 5/21/70

3. CFR Title 49 Parts 170-199.

COMMENTS

It is understood that the charges are covered under a program sponsored by ERDA. This request for services shall not be construed as a purchase request and cannot be used to collect charges from the Air Force Institute of Technology or the U. S. Air Force.

REQUEST FOR REACTOR OPERATION NRL — 1666

Date 11/16/77

Page _____ of _____

ofc Rx Op
11/16/77

ABSTRACT

Irradiate two laser diodes in CIF for 10 minutes each (separately). Irradiation will be inside a polystyrene cylinder that is 17 inches long and 1.25 inches in diameter. A 1 inch by 0.5 inch liner of 0.040 inch cadmium will be placed in the bottom of the container and the entire assembly will be filled with liquid nitrogen (54.7 cc). Nickel flux wires will be placed in the liner.

Reactivity effect of 14.9 gm of cadmium in this configuration based on -0.24% for the 19.4 gm cylinder used before is

$$\frac{-0.24\%}{19.4g} \times 14.9g = -0.18\%$$

Reactivity effect should be slightly less negative than this because of the moderating effect of the polystyrene. An approach to critical experiment will be performed to verify the reactivity. Sample will be periodically removed during approach to critical to check Δk_2 level.

HAZARD ANALYSIS

54.7 cm^3 of liquid nitrogen:

Reaction	$t_{\frac{1}{2}}$	Activity(uCi)
$^{14}N(n,p)^{14}C$	5730 y	0.16
$^{15}N(n,\gamma)^{16}N$	7.13 s	2.86

Assume one MeV gamma per decay:

$$E.R. = 56xA = (56)x(3.02x10^{-6}) = 169 \times 10^{-6} \text{ R/hr}$$

Sample will be raised 10 ft above the core and allowed to decay for 5 half-lives of ^{16}N before removing from CIF.

Exposure from polystyrene will be negligible.

VITA

Thomas Edward Walsh, Jr. was born in Knoxville, Tennessee, on 16 April 1947. He graduated from Knoxville Central High School in 1965, and then attended Carson-Newman College in Jefferson City, Tennessee, from which he received the Bachelor of Science Degree with a major in physics in May of 1969. He attended Air Force Officer Training School in November of 1969 and was assigned to Craig Air Force Base, Alabama. After graduation from pilot training, he served as a pilot in an EB-57 squadron and then as an instructor in Undergraduate Pilot Training. He entered the School of Engineering, Air Force Institute of Technology in June of 1976.

Permanent Address: 5604 Stonycroft Ln
Knoxville, Tn 37918

This thesis was typed by Linda Minteer

UNCLASSIFIED

SECURITY CLASSIFICATION OF THIS PAGE (When Data Entered)

REPORT DOCUMENTATION PAGE		READ INSTRUCTIONS BEFORE COMPLETING FORM
1. REPORT NUMBER GNE/PH/78-11	2. GOVT ACCESSION NO.	3. RECIPIENT'S CATALOG NUMBER
4. TITLE (and Subtitle) EFFECTS OF NEUTRON RADIATION ON ALUMINUM-GALLIUM-ARSENIDE LASERS		5. TYPE OF REPORT & PERIOD COVERED MS THESIS 6. PERFORMING ORG. REPORT NUMBER
7. AUTHOR(s) Thomas E. Walsh, Jr. Capt USAF		8. CONTRACT OR GRANT NUMBER(s)
9. PERFORMING ORGANIZATION NAME AND ADDRESS Air Force Institute of Technology (AFIT-ENP) Wright-Patterson AFB, Ohio 45433		10. PROGRAM ELEMENT, PROJECT, TASK AREA & WORK UNIT NUMBERS
11. CONTROLLING OFFICE NAME AND ADDRESS Air Force Weapons Laboratory Kirtland AFB, New Mexico 87115		12. REPORT DATE March 1978 13. NUMBER OF PAGES 55
14. MONITORING AGENCY NAME & ADDRESS(if different from Controlling Office) Air Force Institute of Technology (AFIT-ENP) Wright-Patterson AFB, Ohio 45433		15. SECURITY CLASS. (of this report) UNCLASSIFIED 15a. DECLASSIFICATION/DOWNGRADING SCHEDULE

16. DISTRIBUTION STATEMENT (of this Report)

Approved for public release; distribution unlimited.

17. DISTRIBUTION STATEMENT (of the abstract entered in Block 20, if different from Report)

18. SUPPLEMENTARY NOTES

Approved for Public Release; IAW AFR 190-17

JERRAL F. GUESS, CAPTAIN USAF
Director of Information

19. KEY WORDS (Continue on reverse side if necessary and identify by block number)

Gallium-Arsenide (GaAs)
Radiation Effects
Aluminum-Gallium-Arsenide (AlGaAs)
Neutron Radiation Effects
Laser Diode
Injection Laser

10 to the 14th power n/sq cm

20. ABSTRACT (Continue on reverse side if necessary and identify by block number)

Double heterojunction aluminum-gallium-arsenide laser diodes were irradiated in a nuclear reactor to determine the effects of neutron radiation. Two types of lasers were used; RCA C30127 and Laser Diode Laboratories LCW-10. Both types can operate continuously at room temperature. Both types of diodes showed significant decreases in power output at neutron fluences of 10^{14} n/cm^2. Linear increases in threshold current and linear decreases in external quantum efficiency were observed. There was no significant change in bias voltage

DD FORM 1 JAN 73 1473 EDITION OF 1 NOV 65 IS OBSOLETE

UNCLASSIFIED

SECURITY CLASSIFICATION OF THIS PAGE (When Data Entered)

 10 to the 15th power n/sq cm

versus forward current or in the spectral composition of the output of the diodes at neutron fluences up to 10^{15} n/cm^2. Formulas were developed to predict the changes in threshold current, external quantum efficiency and power at a constant current above threshold. Damage coefficients for these formulas were derived from the irradiation data. Unusual discontinuities were observed in the power output versus input current curves of some diodes. Neutron irradiation tended to enhance these anomalies.